Carbohydrate Polymers 83 (2011) 528–536

Contents lists available at ScienceDirect

Carbohydrate Polymers

journal homepage: www.elsevier.com/locate/carbpol

Comparative and competitive adsorption of copper, lead, and nickel using chitosan immobilized on bentonite

Cybelle Morales Futalan[a], Chi-Chuan Kan[b], Maria Lourdes Dalida[c], Kuo-Jung Hsien[b], Chelo Pascua[d], Meng-Wei Wan[b,*]

[a] Department of Environmental Engineering, University of Philippines-Diliman, Quezon City 1800, Philippines
[b] Department of Environmental Engineering and Science, Chia Nan University of Pharmacy and Science, Tainan 71710, Taiwan
[c] Department of Chemical Engineering, University of Philippines-Diliman, Quezon City 1800, Philippines
[d] National Institute of Geological Sciences, University of Philippines-Diliman, Quezon City 1800, Philippines

ARTICLE INFO

Article history:
Received 13 May 2010
Received in revised form 30 July 2010
Accepted 9 August 2010
Available online 17 August 2010

Keywords:
Antagonistic
Adsorption
Chitosan
Bentonite
Comparative and competitive

ABSTRACT

The comparative and competitive adsorption of Cu(II), Ni(II), and Pb(II) from aqueous solution using chitosan immobilized on bentonite (CHB) was investigated. The adsorption data of single and binary systems indicated that Cu(II) and Pb(II) best fits Freundlich isotherm while Ni(II) follows Langmuir. In binary systems, a decrease in adsorption capacities and isotherm constants was observed, showing preference of adsorption in the order of Pb(II) > Cu(II) > Ni(II). Kinetic studies of single system indicated that the pseudo-second order is the best fit with high correlation coefficients ($R^2 > 0.99$) and low sum of error values (SE = 0.13–0.46%). Thermodynamic studies illustrated that adsorption of CHB are exothermic and causes a decrease in the entropy. The adsorption of Pb(II) is spontaneous while Ni(II) is non-spontaneous at 25–55 °C. Cu(II) adsorption is only spontaneous at 25 °C.

1. Introduction

Heavy metals contamination in wastewater is mainly contributed by anthropogenic sources like electronics assembly and fabrication, battery manufacturing, paper and pulp industries, metal fabrication, and mining activities (Sari, Tuzen, Citak, & Soylak, 2007). Philippines is included in the top 30 World Metal Statistics in terms of Cu(II) and Ni(II) production. According to the Philippine Clean Water Act 2004 RA 9275, the ore mining and processing of Cu(II) and Ni(II) produce Pb(II) in their wastewaters.

Cu(II) and Ni(II) are essential nutrients needed by the body in trace amounts. However, an increase in the intake of Cu(II) can cause health problems like gastrointestinal disturbance, and liver and kidney failure while high Ni(II) intake can lead to birth defects, embolism, and chronic bronchitis (Han et al., 2009). On the other hand, Pb(II) has no essential function to the human body but has several unwanted effects like kidney damage, and disruption of the nervous system. In addition, the presence of heavy metals at elevated levels in surface water and groundwater environment also prevents any beneficial use of the water bodies. Therefore, it is essential to control the concentration of heavy metals in wastewaters before its disposal into the environment.

Common removal technologies of heavy metals are membrane separation, ion exchange, electro deposition, and chemical precipitation. These methods proved to be costly and inept, especially in removing trace amounts of heavy metals (Popuri, Vijaya, Boddu, & Abburi, 2009). Another disadvantage is the production of sludge or mud, which requires proper disposal and confinement (Rhazi et al., 2002). On the other hand, adsorption effectively removes contaminants in wastewater with high solute loadings and even at dilute concentrations (<100 mg/L). Use of natural adsorbents like peat, banana pith, rice hull and chitosan prove to be economical and effective in removing a variety of contaminants (Popuri et al., 2009; Septhum, Rattanaphani, Bremner, & Rattanaphani, 2007).

Chitosan contains reactive hydroxyl (–OH) groups and amino ($–NH_2$) groups that have the potential to bind heavy metals. Pure chitosan tends to agglomerate and form a gel in aqueous media, rendering most of the hydroxyl and amino groups inaccessible for metal binding. Coating chitosan as a thin layer onto an immobilization support increases the accessibility of its binding sites, and improves the mechanical stability (Wan, Petrisor, Lai, Kim, & Yen, 2004; Wan, Kan, Rogel, & Dalida, 2010). Chitosan support materials that have been previously studied are sand for Cu(II) & Pb(II) removal (Wan et al., 2010), calcium alginate beads for Ni(II) removal (Vijaya, Popuri, Boddu, & Krishnaiah, 2008), alumina for Cr(VI) removal (Veera, Krishnaiah, Jonathan, & Edgar, 2003), and PVC beads for Cu(II) and Ni(II) removal (Popuri et al., 2009). Clay

* Corresponding author. Tel.: +886 6 266 0615; fax: +886 6 213 1291.

0144-8617/$ – see front matter © 2010 Elsevier Ltd. All rights reserved.
doi:10.1016/j.carbpol.2010.08.013

presents as a promising support material due to its mechanical and chemical stability, low cost, and availability (Gecol, Miakatsindila, Ergican, & Hiibel, 2006; Wang & Wang, 2008). Several studies have been performed on montmorillonite/chitosan composites for the removal of tannic acid (An & Dultz, 2007), dyes (Monvisade & Sirriphannon, 2009), and tungsten (Gecol et al., 2006). Using a geologically available support material lessens the amount of chitosan to be used in synthesizing the composite material. Therefore, it is practical to use it as a possible material for permeable reactive barrier in the treatment of acidic plumes and contaminated groundwater.

In this investigation, chitosan immobilized on bentonite (CHB) is characterized using TG and BET analysis. The main objective of the study is to determine the capacity of CHB in removing Pb(II), Cu(II), and Ni(II) from aqueous solution under static conditions. It aims to determine the maximum adsorption capacity of CHB in single and binary solutions, to establish the applicable isotherm model, to illustrate the suitable kinetics mechanism, and to determine the thermodynamic parameters.

2. Materials and methods

2.1. Materials and equipment

Chitosan, low molecular weight and with 75–85% degree of deacytelation, was obtained from Sigma–Aldrich. Bentonite was procured from Ridel-de Haën while HCl (37% fuming), and ICP multi-element standard solution were from Merck Germany. Analytical grade of $Cu(NO_3)_2{\cdot}2.5H_2O$, $Pb(NO_3)_2$ and $Ni(NO_3)_2{\cdot}6H_2O$ were procured from Ridel-de Haën. A Channel Precision Oven model DV452 220 V was used for drying the CHB adsorbent. A BT-350 reciprocal shaker bath was utilized for the batch studies. Metal analysis was done using inductively coupled plasma optical emission spectrometry (ICP-OES) Perkin Elmer DV2000 Series. Surface area analysis was performed using the Brunauer, Emmett, and Teller (BET) multipoint technique using N_2 adsorption at 77 K. The thermogravimetric curves of chitosan, bentonite and CHB were obtained using a Perkin Elmer Pyris diamond thermomechanical analyzer with a heating rate of 10 °C min^{-1}.

2.2. Preparation of chitosan immobilized on bentonite

About 5 g of chitosan was dissolved in 300 mL of 5% (v/v) HCl in a magnetic plate by stirring the solution for 2 h at 300 rpm. Bentonite (100 g) was slowly added into the solution and was stirred for another 3 h. The solution was added with 1 N NaOH in a dropwise method until neutralization is reached. The adsorbent was washed with deionized water, dried in the oven at 65 °C for 24 h, pulverized, and sieved. Adsorbent with particle size ranging from 0.50 mm to 0.21 mm was used in the batch studies.

2.3. Adsorption kinetic studies

Single and binary metal solutions of Cu(II), Ni(II) and Pb(II) were prepared with concentrations of 25 mg/L and 200 mg/L, respectively. Adjustment of pH was done using 0.1 N NaOH or 0.1 N HCl. The initial pH of the solution was set at pH 4, making it similar to the pH of mining wastewaters, which are typically acidic (pH 4–6).

An Erlenmeyer flask is filled with 0.2 g CHB and 30 mL of the metal solution. The metal solution was agitated using a reciprocal shaker bath that was maintained at 50 rpm and the pre-determined contact times ranged from 1 min up to 24 h. The solution is filtered using a Whatman #40 filter paper. The filtrate was analyzed using ICP-OES using wavelengths 324.75 nm, 231.60 nm, and 220.35 nm for Cu(II), Ni(II), and Pb(II), respectively.

The adsorption capacity was calculated:

$$q_e = \frac{(C_0 - C_e)V}{W} \quad (1)$$

where C_0 is the initial metal concentration (mg/L), C_e is the final or equilibrium concentration (mg/L), V is the volume of the metal solution (mL), and the W is the weight of CHB (g).

2.4. Adsorption isotherm studies

Single and binary metal solutions of Cu(II), Ni(II), and Pb(II) with concentrations of 50–500 mg/L were utilized for isotherm studies. The experiments were performed using 0.2 g of CHB in 30 mL of the metal solution in an Erlenmeyer flask. Solutions with an initial pH 4 were agitated using a reciprocal shaker bath at 50 rpm for 24 h at room temperature.

2.5. Adsorption thermodynamics studies

The thermal effects were studied under four different temperatures: 25 °C, 35 °C, 45 °C, and 55 °C. The thermodynamic studies were conducted with initial concentration of 300 mg/L of Cu(II), Ni(II), and Pb(II) solutions at pH 4 and were agitated using a reciprocal shaker bath for 24 h at a speed of 50 rpm.

3. Results and discussions

3.1. Surface area analysis

The physical characteristics of bentonite, chitosan and CHB are listed in Table 1. The total porosity is classified into three categories according to the pore diameter (d). The categories are: macropores ($d > 50$ nm), mesopores ($2 < d < 50$ nm), and micropores ($d < 2$ nm). Based on Table 1, bentonite, chitosan, and CHB are mesoporous. The surface area, total pore volume and micropore volume values are arranged in the following sequence: bentonite > CHB > chitosan. The lower surface area and pore volume of CHB was due to the chitosan molecules blocking the pores of bentonite. In addition, agglomeration of chitosan with bentonite was caused by bridging mechanisms and interaction of the hydroxylated edges of bentonite with each other.

3.2. TG analysis

The thermogravimetric profiles of bentonite, chitosan and CHB are depicted in Fig. 1. Bentonite has two major weight loss patterns: 90–120 °C, which corresponds to the evaporation of adsorbed water, and 500–700 °C, which is caused by the loss of structure of the hydroxyl group. Moreover, chitosan has two stages of weight loss: 70–100 °C, which is the loss of adsorbed water. The second major weight loss starts around 243 °C, then chitosan was burnt out completely at 570 °C. The thermogram of CHB is similar to that of bentonite, with a slightly higher weight loss. This indicates that 3.1% of chitosan has successfully coated onto bentonite.

Table 1
Surface area determination of the bentonite, chitosan, and CHB.

	Chitosan	Bentonite	CHB
BET surface area (m^2/g)	2.12	84.28	33.17
Langmuir surface area (m^2/g)	2.39	86.33	35.09
Micropore area (m^2/g)	0.38	33.73	12.45
Average pore diameter (nm)	11.61	5.72	8.54
Total pore volume (cm^3/g)	0.032	0.085	0.048

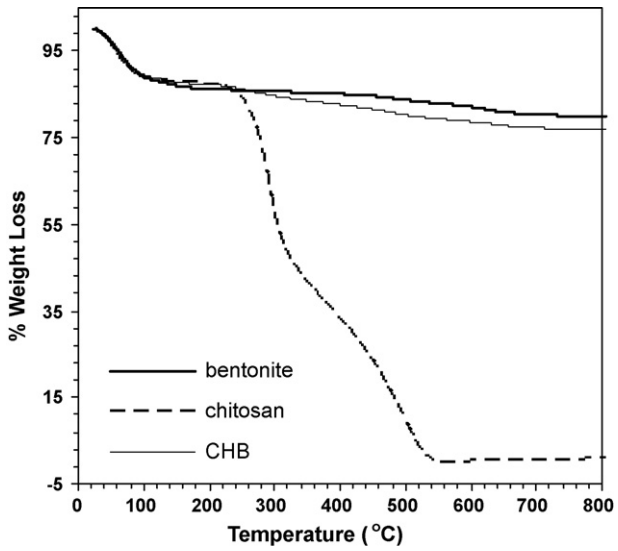

Fig. 1. Thermogravimetric curves of bentonite, chitosan, and CHB.

3.3. Effect of contact time on the adsorption capacity of single and binary metal solutions

Fig. 2(a) shows the adsorption capacity, q_t of single metal solutions graphed against time. The same trend was observed for Cu(II), Ni(II) and Pb(II), where the initial stages is indicated by a steep increase in q_t. At the start, there was an abundance of hydroxyl and amino functional groups available for binding and the metal concentration present in the solution is high. As it nears equilibrium, the functional groups are almost occupied by metals. The adsorbent surface becomes difficult to be filled in owing to the repulsive forces between the metal ions bound on the CHB and the metal ions still present in the solution.

For Pb(II), Cu(II), and Ni(II), equilibrium is attained in 1 h for 25 mg/L solution and 4 h for the 200 mg/L solution. A lower concentration means lesser amount of metal ions competes to be adsorbed, resulting to an early attainment of equilibrium. Increasing the initial concentration means higher amount of metal ions resulting to a tighter competition in binding to the functional groups of CHB. The effect of steric crowding also contributes to a delay in reaching equilibrium, due to the repulsive forces caused by the shorter distances between metal ions at high concentrations.

At 25 mg/L, Pb(II), Cu(II), and Ni(II) have similar maximum adsorption capacities indicating the concentration is too low to saturate all functional groups of the CHB. At 200 mg/L concentration, Pb(II) with 28.77 mg/g exhibited the highest capacity to be adsorbed over Cu(II) with 20.90 mg/g and Ni(II) with 12.35 mg/g, respectively.

The maximum adsorption capacities of binary systems Pb–Ni, Pb–Cu, and Cu–Ni were determined. Actual wastewater is a mixture of different metals. The following combinations were tested to examine the effect of each metal on each other in terms of their adsorption capacities.

Fig. 2(b–d) indicates the adsorption capacity of binary system Pb–Ni, Pb–Cu and Cu–Ni, respectively. Equilibrium is delayed in binary systems, where it is reached around 4 h for 25 mg/L and 6 h for 200 mg/L, respectively. The adsorption capacities in binary systems decreased considerably in comparison to single system values, indicating a strong competition between the metal ions in binding to the functional groups of CHB. Moreover, in the Pb–Ni system, the adsorption capacity of Ni(II) decreased to 1.06–1.22 times while Pb(II) uptake decreased a maximum of 1.52 times at 200 mg/L but seems unaffected at 25 mg/L, when compared to single system values. However, the Pb–Cu system illustrates a significant decrease in the adsorption capacity for Pb(II) (1.1–1.93 times) and Cu(II) (1.17–1.48 times) at both concentrations. In Cu–Ni system, the adsorption capacity of Cu(II) and Ni(II) decreased to 1.06–1.44 times and 1.32–1.81 times, respectively. The adsorption capacity of Pb(II) is observed to be more negatively affected in the presence of Cu(II) over Ni(II). In binary systems, Pb(II) is always favorably adsorbed over Cu(II) and Ni(II), which is consistent with the results in the single metal systems. Previous studies on competitive adsorption have similar results in terms of selectivity in a multi-metal solution, where Pb(II) is favorably adsorbed over Cu(II) using valonia tannin resin (Ahyan Sengil & Ozacar, 2009), Sargassum biomass (Virjayaghavan, Teo, Balasubramanian, & Joshi, 2009), and peat (Qin et al., 2006) while Cu(II) is preferably removed over Ni(II) using chitosan-coated perlite beads (Swayampakula, Boddu, Nadavala, & Abburi, 2009).

3.4. Chitosan-coated bentonite selectivity in removing Cu(II), Ni(II), and Pb(II)

In single and binary metal systems, Pb(II) has the highest adsorption capacity over Cu(II) and Ni(II). This is influenced by the electronegativity value of a metal ion, where the values are arranged in the order: Pb(II) (2.33) > Cu(II) (1.95) > Ni(II) (1.91) (Virjayaghavan et al., 2009). There is more attraction between two atoms when their electronegativity difference is large. Pb(II) being the most electronegative, results to its preferential adsorption to the hydroxyl (–OH) and amino ($-NH_2$) groups of CHB over Cu(II) and Ni(II) accordingly.

3.5. Kinetics for single metal solutions

To identify what type of adsorption mechanism occurs, the kinetic equations namely pseudo-first order, pseudo-second order and intraparticle diffusion were utilized. The kinetic rate constants were also determined.

The pseudo-first order equation takes the linearized form:

$$\log\ (q_e - q_t) = \log\ q_e - \frac{k_1 t}{2.303} \tag{2}$$

where k_1 (min^{-1}) is the pseudo-first order kinetic constant, q_t (mg/g) is the adsorption capacity at time t (Hameed, Tan, & Ahmad, 2008).

The pseudo-second order kinetic equation is given by:

$$\frac{t}{q_t} = \frac{1}{k_2 q_e^2} + \frac{t}{q_e} \tag{3}$$

where k_2 (g/mg min) is the kinetic constant (Hameed et al., 2008).

The third kinetic equation is the intraparticle diffusion model, given by the equation:

$$q_t = k_i t^{0.5} + C_i \tag{4}$$

where k_i ($\text{mg g}^{-1}\text{min}^{-1.5}$) is the rate constant of intraparticle diffusion controlled sorption, and C_i is the thickness of the boundary layer (Hameed et al., 2008).

Table 2 indicates the kinetic constants as well as the correlation coefficients, R^2. The plots for pseudo-first and intraparticle diffusion have low correlation coefficient values, which implies that neither of the two is the rate-limiting step. Pseudo-second order equation has the highest correlation coefficient for all three metals ($R^2 > 0.99$), implying that chemisorption is the rate controlling mechanism. This indicates that a covalent bond is formed through sharing of electrons between the metal ion and the CHB adsorbent (Chen, Yang, & Chen, 2009). The pseudo-second order rate constants, k_2 have higher values at lower concentrations. A low con-

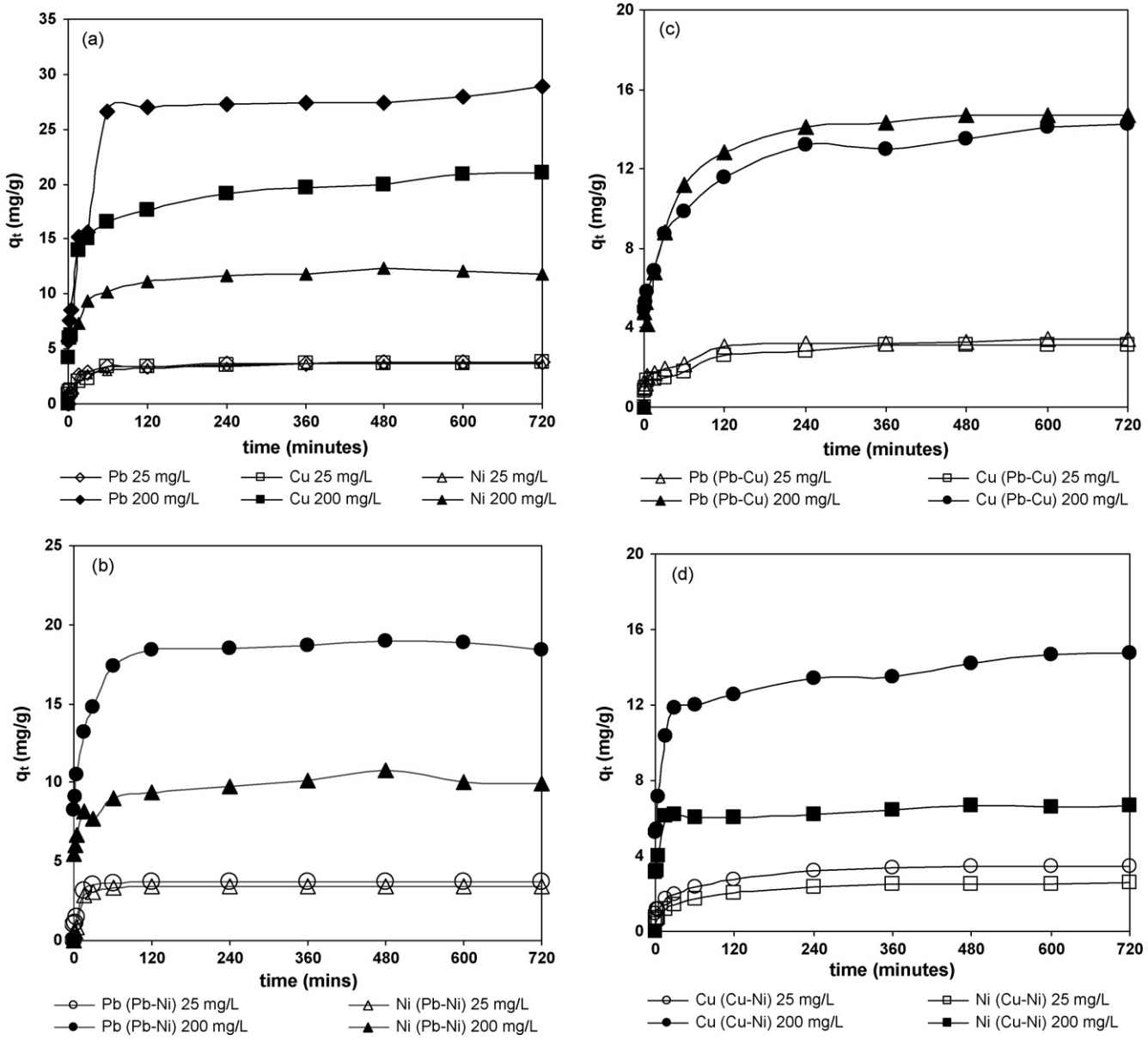

Fig. 2. Adsorption capacity against contact time of (a) single system of Cu(II), Ni(II), and Pb(II); (b) binary Pb–Ni system; (c) binary Pb–Cu system; (d) binary Cu–Ni system.

centration means less competition between metal ions in binding to the functional groups, thus heavy metals are adsorbed quickly.

Table 3 compares the theoretical and experimental values of the adsorption capacity of Pb(II), Cu(II), and Ni(II) in single metal systems. The sum of errors (SE%) is computed using the equation:

$$\mathrm{SE\%} = \frac{100}{n-1}\sum \frac{|q_{\mathrm{exp}} - q_{\mathrm{theo}}|}{q_{\mathrm{exp}}} \quad (5)$$

where q_{exp} is the experimental adsorption capacity (mg/g), n is the number of data points, and q_{theo} is the theoretical adsorption capacity (mg/g) obtained from the pseudo-first and pseudo-second plots, respectively (Bakouri, Usero, Morillo, & Ouassini, 2009). The experimental and theoretical values for the pseudo-second order equation are very similar, indicated by very low SE% values (0.13–0.46%) in comparison to the pseudo-first order equation with values from 7.83% to 9.56%. In Fig. 3, the experimental data points

Table 2
Kinetic parameters for pseudo-first order, pseudo-second order and intraparticle diffusion mechanism of single metal systems.

Metal	C_0	Pseudo-first		Intraparticle		Pseudo-second	
		k_1 (min^{-1})	R^2	k_i ($\mathrm{mg/g\,min}^{0.5}$)	R^2	k_2 (g/mg min)	R^2
Pb	25 ppm	0.0122	0.7864	0.2140	0.7207	0.0297	0.9984
	200 ppm	0.0157	0.7686	1.6509	0.8326	0.0032	0.9937
Cu	25 ppm	0.0117	0.7699	0.2491	0.7946	0.0325	0.9974
	200 ppm	0.0157	0.9072	1.0926	0.7881	0.0060	0.9989
Ni	25 ppm	0.0106	0.7941	0.1896	0.7305	0.0344	0.9985
	200 ppm	0.0099	0.9087	0.4411	0.8963	0.0148	0.9985

Table 3
Comparison of experimental and theoretical adsorption capacities of pseudo-first order, and pseudo-second order of single metal systems.

Metal	C_0	q_{exp} (mg/g)	Pseudo-first		Pseudo-second	
			q_{theo} (mg/g)	% Error	q_{theo} (mg/g)	% Error
Pb	25 *ppm*	3.75	1.89	8.27	3.72	0.13
	200 ppm	28.00	14.85	7.83	28.65	0.39
Cu	25 *ppm*	3.65	1.88	8.08	3.59	0.27
	200 ppm	20.00	10.58	7.85	20.28	0.23
Ni	25 *ppm*	3.62	1.82	8.29	3.52	0.46
	200 rpm	12.29	5.24	9.56	11.83	0.62

Table 4(a)
Percent (%) removal and adsorption capacity values of Pb(II), Cu(II), and Ni(II) at different temperatures.

Temperature (°C)	% Removal			Adsorption capacity, q_t (mg/g)		
	Pb	Cu	Ni	Pb	Cu	Ni
25	80.00	51.41	39.04	36.01	23.11	17.51
35	75.41	45.10	36.23	33.97	20.29	16.28
45	75.09	43.12	34.03	33.76	19.40	15.31
55	72.41	40.82	32.34	32.55	18.37	14.53

of Cu(II), Ni(II) and Pb(II) are in good agreement with the non-linear plots generated using the pseudo-second order equation. This further validates that the pseudo-second order best describes the kinetic data.

3.6. Thermodynamics of single metal systems

The effect of temperature from 25 °C to 55 °C on the removal efficiency of CHB using 300 mg/L of Cu(II), Ni(II), and Pb(II) was investigated. Table 4(a) shows the effect of increasing temperature slightly decreases % removal and adsorption capacity for Pb(II), Cu(II), and Ni(II). From the trend, the decrease of the uptake of metal ions by the CHB at higher temperature indicates that the adsorption is an exothermic process.

The thermodynamic parameters like free Gibbs energy (ΔG^0), enthalpy (ΔH^0), and entropy (ΔS^0) are shown in Table 4(b). The constants were computed using the following equations:

$$K_c = \frac{C_{ads}}{C_e} \tag{7}$$

$$\Delta G^0 = -RT \ \ln K_c \tag{8}$$

$$\ln K_c = \frac{\Delta S^0}{R} - \frac{\Delta H^0}{RT} \tag{9}$$

where K_c is the equilibrium constant, C_{ads} is the amount metal adsorbed by the CHB (mg/L) at equilibrium, C_e is the amount of metal remaining in the solution (mg/L) at equilibrium, R is the universal gas constant (kJ/mol K), and T is the solution temperature (K) (Sari et al., 2007).

Table 4(b)
Thermodynamic constant parameters for Cu(II), Ni(II) and Pb(II) single systems.

Metal	Temperature (°C)	ΔG^0 (kJ/mol)	ΔH^0 (kJ/mol)	ΔS^0 (J/mol K)
Pb	25	−3.4350	−10.4713	−0.0234
	35	−2.8698		
	45	−2.9176		
	55	−2.6322		
Cu	25	−0.1398	−11.1623	−0.0374
	35	0.5041		
	45	0.7328		
	55	1.0129		
Ni	25	1.1042	−7.9387	−0.0304
	35	1.4479		
	45	1.7509		
	55	2.0132		

From 25 °C to 55 °C, the values of ΔG^0 for Pb(II) are negative indicating adsorption is spontaneous while the positive ΔG^0 values for Ni(II) mean the process is non-spontaneous. Cu(II) adsorption is only spontaneous at 25 °C but is non-spontaneous from 35 °C to 55 °C. This supports why the adsorption capacity of Pb(II) is higher than Cu(II) and Ni(II) because the more negative the ΔG^0 value, the more spontaneous and more favorable the adsorption. Increasing the temperature results to a less negative value of ΔG^0 that indicates the reaction becomes less spontaneous. This is supported by the fact that Pb(II), Cu(II), and Ni(II) have negative ΔH^0 values. It signifies that the adsorption process is exothermic; hence increasing the temperature resulted to a decrease in the metal adsorption capacity. The negative ΔS^0 values signify there is a decrease in the randomness at the solid-solution interface of Pb(II), Cu(II), and Ni(II) onto CHB surface (Chiou & Li, 2003).

3.7. Adsorption isotherms of single metal solutions

To further understand adsorption of Cu(II), Ni(II), and Pb(II) onto the CHB, it is important to know how much heavy metal is adsorbed. The capacity of CHB is calculated using the adsorption isotherm models namely Langmuir, Freundlich and Dubinin–Radushkviech (D–R) equations.

The Langmuir isotherm is one of the models that describe monolayer coverage. It assumes a homogenous adsorption surface with binding sites having equal energies (Chiou & Li, 2003). The linearized form of Langmuir is:

$$\frac{1}{q_e} = \frac{1}{q_{mL}} + \frac{1}{bq_{mL}C_e} \tag{10}$$

where q_e is the adsorption capacity at equilibrium (mg/g), C_e is the equilibrium concentration of the metal ion in the solution (mg/L), q_{mL} (mg/g) and b (L/mg) represents maximum sorption capacity corresponding to complete the monolayer coverage and affinity of the heavy metals to the binding sites on the adsorbent, respectively (Vijaya et al., 2008).

The Freundlich equation is an isotherm model illustrating the adsorbent surface to be heterogenous (Kamari & Ngah, 2009). The Freundlich equation has the linear form:

$$\log q_e = \log K_F + \frac{1}{n} \log C_e \tag{11}$$

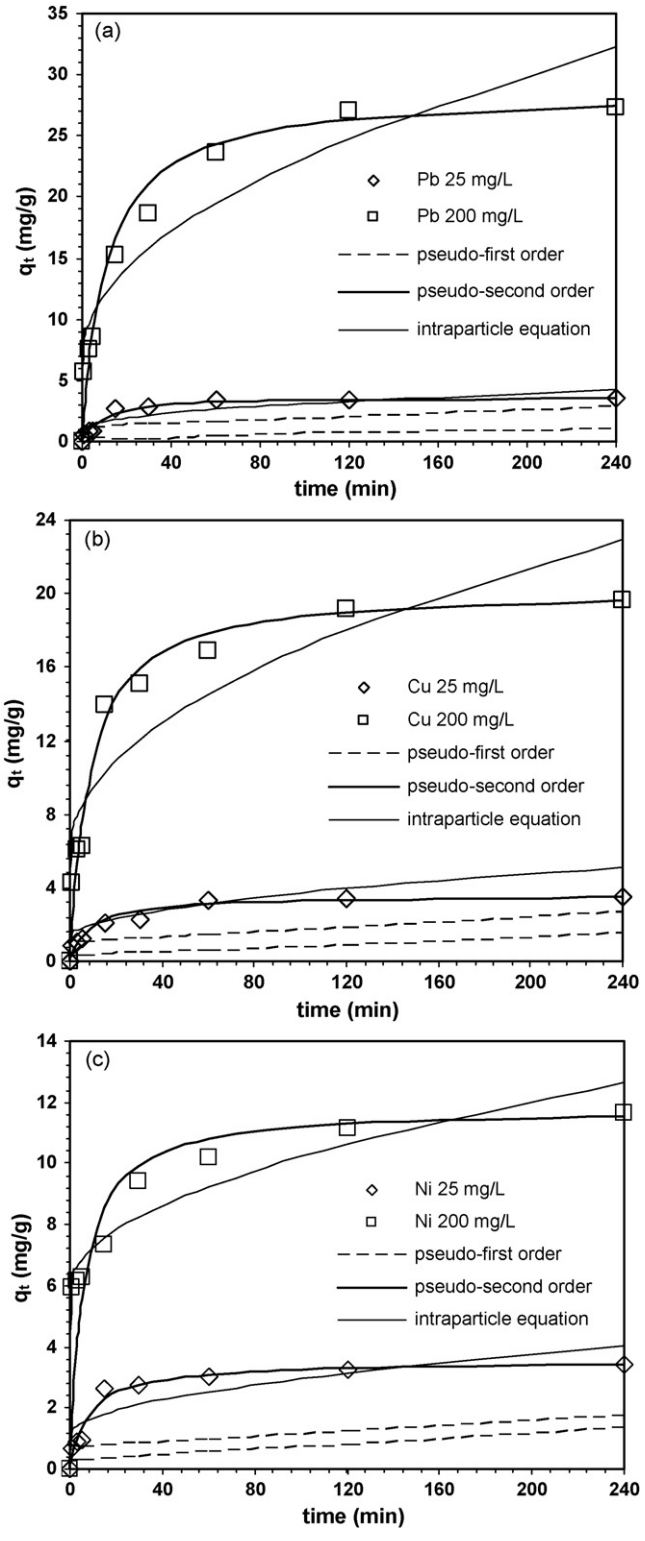

Fig. 3. The kinetic experimental data points of (a) Pb(II), (b) Cu(II), and (c) Ni(II) fitted for pseudo-first order, pseudo-second order and the intraparticle diffusion equation.

where K_F is the maximum adsorption capacity of metal ions and $1/n$ indicates the intensity of metal ions on the adsorbent.

The D–R equation helps in distinguishing if the adsorption process is physical or chemical in nature (Kamari & Ngah, 2009). It is given by the equation:

$$\ln q_e = \ln q_m - \beta\varepsilon^2 \tag{12}$$

where q_m is the maximum amount of metal ion adsorbed onto unit weight of the adsorbent (mmol/g), β is a constant that is related to the adsorption energy (mol^2/kJ^2) and ε is the Polanyi potential, which is given by the equation:

$$\varepsilon = RT \ln\left[1 + \frac{1}{C_e}\right] \tag{13}$$

where R is the universal gas constant (kJ/mol K), and T is the absolute operating temperature (K). In solving for q_m and β, $\ln q_e$ is graphed against ε^2.

The calculated Langmuir, Freundlich, and D–R constants are shown in Table 5(a). Pb(II) and Cu(II) have high correlation values ($R^2 > 0.99$) for Freundlich isotherm while Ni(II) provided a better fit with Langmuir isotherm. The Langmuir isotherm constants, q_{mL} and b, follows the order of Pb(II) > Cu(II) > Ni(II). Pb(II) having the highest b value means the highest affinity to bind to the functional groups, resulting to maximum monolayer adsorption capacity over Cu(II) and Ni(II). For the Freundlich constants, Pb(II) have the highest K_F and $1/n$ values over Cu(II) and Ni(II), respectively. Pb(II) having the lowest $1/n$ value means it has the highest affinity to the functional groups of CHB resulting to a high K_F.

The q_{mL} values of Langmuir are similar to the q_m values derived from D–R isotherm model. The similarities of the values cannot be clarified since the two isotherms are based on different mechanisms. Langmuir describes the mechanism between the adsorbate and the surface of the adsorbent whereas D–R describes the relationship between the adsorbent and the volume of adsorbate that occupy the micropores of the adsorbent (Oh, Kwak, & Shin, 2009).

The Langmuir constant, b is used to calculate R_L, a dimensionless separation factor given by the equation:

$$R_L = \frac{1}{1 + bC_0} \tag{14}$$

where C_0 is the initial concentration (mg/L). R_L values will tell if the adsorption is unfavorable ($R_L > 1$), linear ($R_L = 1$), favorable ($0 < R_L < 1$), or irreversible ($R_L = 0$) (Sari et al., 2007). The R_L values at concentrations 50–500 mg/L for Pb(II) (0.0002–0.0020), Cu(II) (0.0268–0.2157), and Ni(II) (0.0490–0.3401), implies that the adsorption is favorable. Therefore CHB is an appropriate adsorbent for the removal of Pb(II), Cu(II), and Ni(II).

3.8. Adsorption isotherms of binary metal solutions

For binary systems, the original Langmuir and Freundlich isotherm equations were applied to determine the effect of presence of another metal ion on the isotherm constants.

In Table 5(b), the isotherm constant values for Pb–Cu, Pb–Ni, and Cu–Ni system are listed. For the Pb–Ni system, Pb(II) best fits Freundlich (0.9878) while Ni(II) has a better correlation coefficient value for Langmuir (0.9507). In the Pb–Cu system, Pb(II) and Cu(II) best fit with Freundlich under values of 0.9905 and 0.9812, respectively. The Cu–Ni system shows that Cu(II) correlates well with Freundlich (0.9753) while Ni(II) follows the Langmuir isotherm (0.9945). Fig. 4 illustrates that the experimental data of single and binary systems for Pb(II) and Cu(II) were an acceptable fit with the non-linear plot of the Freundlich model while the data points for Ni(II) were in good agreement with the predicted Langmuir model. The isotherm models followed by Pb(II), Cu(II), and Ni(II) whether it is a single or binary system are the same. All binary systems of Pb–Ni, Pb–Cu, and Cu–Ni have their adsorption capacity values follow the same selectivity order observed in single metal systems: Pb(II) > Cu(II) > Ni(II).

Table 6 shows a comparison of the isotherm constant values in single and binary systems. The q^0 and $q_{m,MIX}$ indicate the Langmuir maximum monolayer capacity in single and binary system, while $K_F{}^0$ and $K_{F,MIX}$ are the Freundlich adsorption capacity

Table 5(a)
Adsorption isotherm model constants for single metal systems.

Metal	Langmuir			Freundlich					
	b	q_{mL}	R^2	$1/n$	K_F	R^2	β	q_m	R^2
Pb	9.9737	26.3852	0.8606	0.2199	14.2594	0.9905	0.0208	28.8613	0.6681
Cu	0.0727	21.5517	0.9587	0.3325	3.8976	0.9966	7.9099	18.8027	0.7317
Ni	0.0388	15.8228	0.9846	0.3235	2.5433	0.9655	28.7780	13.2712	0.8168

Table 5(b)
Adsorption isotherm model constants for binary metal systems.

Metal	Langmuir			Freundlich		
	b	q_{mL}	R^2	$1/n$	K_F	R^2
Pb (Pb–Ni)	0.5919	20.8333	0.8680	0.2465	7.2410	0.9878
Ni (Pb–Ni)	0.0417	12.6103	0.9507	0.2860	2.4643	0.8939
Pb (Pb–Cu)	0.1137	18.0832	0.8754	0.3124	3.8887	0.9905
Cu (Pb–Cu)	0.0781	17.0940	0.8600	0.3435	3.0227	0.9812
Cu (Cu–Ni)	0.0265	15.3846	0.9775	0.3243	3.4610	0.9753
Ni (Cu–Ni)	0.0154	8.6806	0.9945	0.3460	1.3002	0.9180

of single metal solution and in the presence of other metals, respectively. The value of $q_{m,MIX}/q^0$ and $K_{F,MIX}/K_F{}^0$ will imply whether the effect of mixing metals in a solution is synergistic ($q_{m,MIX}/q^0$ and $K_{F,MIX}/K_F{}^0 > 1$), no net interaction ($q_{m,MIX}/q^0$ and $K_{F,MIX}/K_F{}^0 = 1$), or antagonistic ($q_{m,MIX}/q^0$ and $K_{F,MIX}/K_F{}^0 < 1$) (Qin et al., 2006). All values for Pb(II), Cu(II), and Ni(II) in the binary systems are observed to have decreased in comparison to single system values. The values of $q_{m,MIX}/q^0$ and $K_{F,MIX}/K_F{}^0$ are less than 1, implying that the adsorption of metal ions is suppressed by the presence of other metals in the solution. An antagonistic effect is exerted by the metal ions on each others' adsorption capacity.

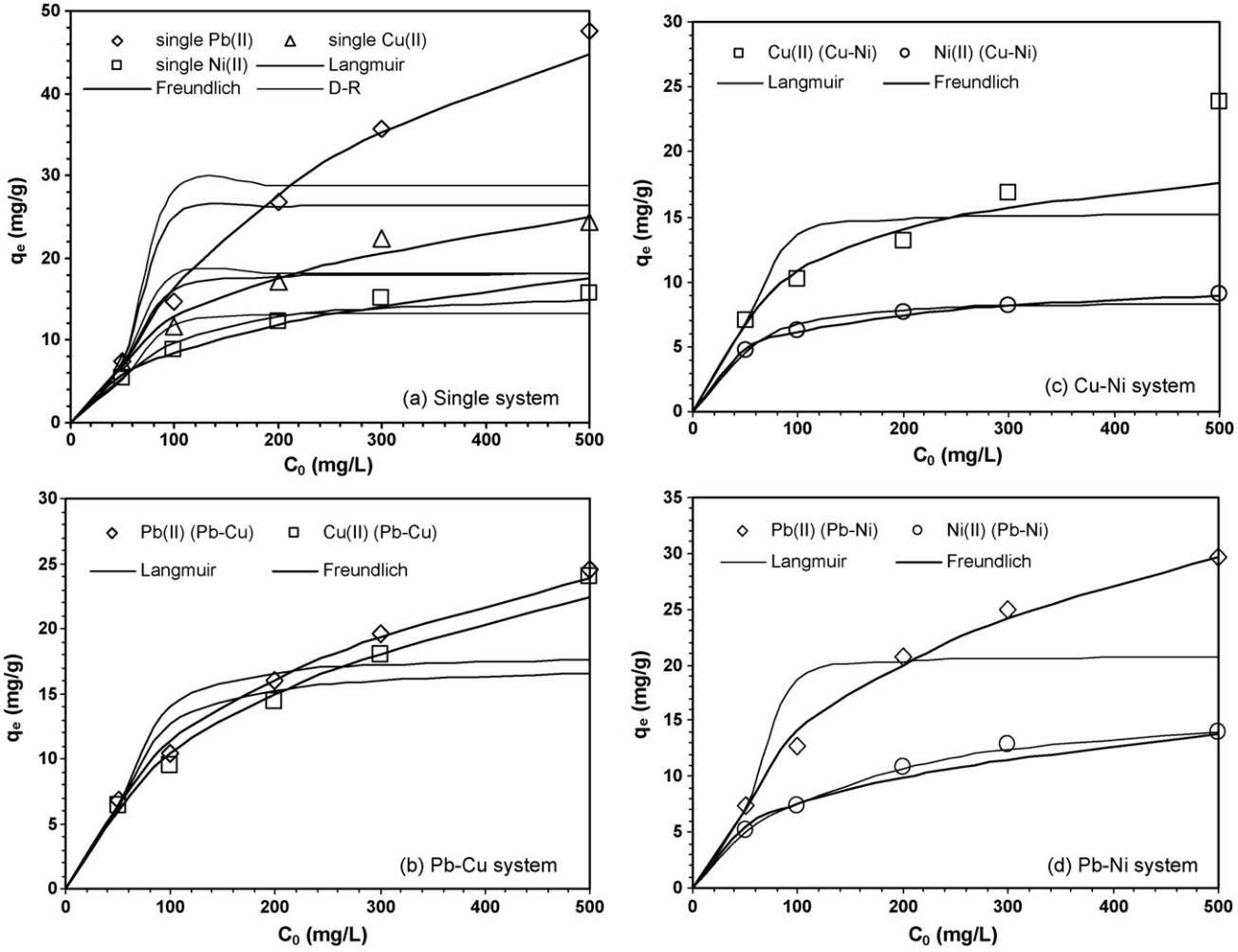

Fig. 4. Comparison of experimental isotherm data of Pb(II), Cu(II), and Ni(II) in single and binary systems against the theoretical non-linear plots generated using the Langmuir, Freundlich and D–R models.

Table 6
A comparison of the Langmuir and Freundlich isotherm constants in single and binary systems.

Metal	Langmuir			Freundlich		
	q^0	$q_{m,MIX}$	$q_{m,MIX}/q^0$	$K_F{}^0$	$K_{F,MIX}$	$K_{F,MIX}/K_F{}^0$
Pb–Ni						
Pb	26.3852	20.8333	0.7895	14.2594	7.2410	0.5078
Ni	15.8228	12.6103	0.7969	2.5433	2.4643	0.9689
Pb–Cu						
Pb	26.3852	18.0832	0.6854	14.2594	3.8887	0.2727
Cu	21.5517	17.0940	0.7932	3.8976	3.0227	0.7755
Cu–Ni						
Cu	21.5517	15.3846	0.7138	3.8976	3.4610	0.8880
Ni	15.8228	8.6806	0.5486	2.5433	1.3002	0.5112

3.9. Adsorption mechanism with Cu(II), Ni(II), and Pb(II)

The binding sites of CHB are the hydroxyl (–OH) and amino ($–NH_2$) groups. The nitrogen of amino group and the oxygen of hydroxyl group have an available pair of electrons that can form coordinated covalent bonds with a metal cation. The oxygen atom in the hydroxyl group has a stronger attraction to its electron lone pairs over the nitrogen atom in the amino group therefore the amino group is more likely to donate the lone pairs to a metal ion (Jin & Bai, 2002).

The initial pH of the metal solutions was set to pH 4, which indicates that 99% of the amino groups of CHB are protonated as illustrated by reaction (1) (Rangel-Mendez, Monroy-Zepeda, Leyva-ramos, Diaz-Flores, & Shirai, 2009; Jin & Bai, 2002).

$$R\text{-}NH_2 + H^+ \leftrightarrow R\text{-}NH_3{}^+ \quad (1)$$

Reactions (2) and (3) occur simultaneously, but reaction (3) occurs at a slower rate than reaction (2). Reaction (3) takes place because of the electrical attraction of M^{2+} (Cu(II), Ni(II), and Pb(II)) is stronger than H^+ in binding with the amino groups. A competitive adsorption takes place, where it is sometimes considered as an ion exchange mechanism (Qin et al., 2006).

$$R\text{-}NH_2 + M^{2+} \leftrightarrow R\text{-}NH_2M^{2+} \quad (2)$$

$$R\text{-}NH_3{}^+ + M^{2+} \leftrightarrow R\text{-}NH_2M^{2+} + H^+ \quad (3)$$

According to the isotherm studies, Ni(II) follows the Langmuir isotherm, indicating that it binds to one type of functional group in CHB, which is the amino group. On the other hand, Pb(II) and Cu(II) follow the Freundlich isotherm. It signifies different interaction mechanism where Pb(II) and Cu(II) bind to the hydroxyl and amino groups on CHB.

4. Conclusion

Adsorption of Cu(II), Ni(II) and Pb(II) has been studied for single and binary systems using CHB as adsorbent. The adsorption capacity is highest for Pb(II) over Cu(II) and Ni(II) for single and binary systems. Comparative and competitive isotherm studies indicated that Ni(II) follows the Langmuir isotherm model while the Freundlich isotherm model is followed by Pb(II) and Cu(II). Isotherm constants are observed to have decreased in values in binary systems, signifying strong competition between the metal ions for the binding sites on CHB. These three metals follow the pseudo-second order equation, indicating chemisorption is the rate-limiting step. Moreover, Cu(II), Ni(II) and Pb(II) adsorption on CHB are exothermic and results to an decrease in entropy. At temperatures 25–55 °C, Pb(II) adsorption is spontaneous while Ni(II) adsorption is non-spontaneous. Cu(II) is non-spontaneous at all temperatures except at 25 °C. Conclusively, these preliminary results illustrate the fundamental support of using CHB to establish inexpensive large-scale barrier filters for the removal of heavy metals contaminations in wastewater or groundwater plumes.

Acknowledgements

The author would like to acknowledge Prof. Teh-Fu Yen, University of Southern California, CA, U.S. for their technical assistance in preparing this manuscript, and Taiwan National Science Council (NSC 99-2221-E-041-017) for their financial support.

References

Ahyan Sengil, I., & Ozacar, M. (2009). Competitive biosorption of Pb^{+2}, Cu^{+2}, and Zn^{+2} ions from aqueous solutions onto valonia tannin resin. *Journal of Hazardous Materials*, *166*, 1488–1494.

An, J. H, & Dultz, S. (2007). Adsorption of tannic acid on chitosan-montmorillonite as a function of pH and surface charge properties. *Applied Clay Science*, *36*, 256–264.

Bakouri, H. E., Usero, J., Morillo, J., & Ouassini, A. (2009). Adsorptive features of acid-treated olive stones for drin pesticides: Equilibrium, kinetic and thermodynamic modeling studies. *Bioresource Technology*, *100*, 4147–4155.

Chen, A., Yang, C., & Chen, C. (2009). The chemically crosslinked metal-complexed chitosans for comparative adsorptions of Cu(II), Zn(II), Ni(II), and Pb(II) ions in aqueous medium. *Journal of Hazardous Materials*, *163*, 1068–1075.

Chiou, M. S, & Li, H. Y. (2003). Adsorption behavior of reactive dye in aqueous solution on chemical cross linked chitosan beads. *Chemosphere*, *50*, 1095–1105.

Gecol, H., Miakatsindila, P., Ergican, E., & Hiibel, S. R. (2006). Bioplymer coated clay particles for the adsorption of tungsten from water. *Desalination*, *197*, 165–178.

Han, R., Zou, L., Zhao, X., Xu, Y., Xu, F., Li, Y., et al. (2009). Characterization and properties of iron oxide-coated zeolite as adsorbent for removal of copper(II) from solution in fixed bed column. *Chemical Engineering Journal*, *149*, 123–131.

Hameed, B. H., Tan, I. A. W., & Ahmad, A. L. (2008). Adsorption isotherm, kinetic modeling and mechanism of 2,4,6-trichlorophenol on coconut-husk based activated carbon. *Chemical Engineering Journal*, *144*, 235–244.

Jin, L., & Bai, R. (2002). Mechanisms of lead adsorption on chitosan/PVA hydrogel beads. *Langmuir*, *18*, 9765–9770.

Kamari, A., & Ngah, W. S. (2009). Isotherm, kinetic, and thermodynamic studies of lead and copper uptake of H_2SO_4 modified chitosan. *Colloids Surface B*, *73*, 257–266.

Monvisade, P., & Sirriphannon, P. (2009). Chitosan intercalated montmorillonite: Preparation, characterization and cationic dye adsorption. *Applied Clay Science*, *42*, 427–431.

Oh, S., Kwak, M. Y., & Shin, W. S. (2009). Competitive sorption of lead and cadmium onto sediments. *Chemical Engineering Journal*, *152*, 376–388.

Popuri, S. R., Vijaya, Y., Boddu, V. M., & Abburi, K. (2009). Adsorptive removal of copper and nickel ions from water using chitosan-coated PVC beads. *Bioresource Technology*, *100*, 194–199.

Qin, F., Wen, B., Shan, X. Q., Vie, Y. N., Liu, T., & Zhang, S. Z. (2006). Mechanisms of competitive adsorption of Pb, Cu, and Cd on peat. *Environmental Pollution*, *144*, 669–680.

Rangel-Mendez, J., Monroy-Zepeda, R., Leyva-ramos, E., Diaz-Flores, P., & Shirai, K. (2009). Chitosan selectivity for removing cadmium (II), copper (II), and lead (II) from aqueous phase: pH and organic matter effect. *Journal of Hazardous Materials*, *162*, 503–511.

Rhazi, M, Desbriereres, J., Tolaimate, A., Rinaudo, M., Vottero, P., & Alagui, A. (2002). Contribution to the study of the complexation of copper by chitosan and oligomers. *Carbohydrate Polymers*, *43*, 1267–1276.

Sari, A., Tuzen, M., Citak, D., & Soylak, M. (2007). Equilibrium, kinetic and thermodynamic studies of adsorption of Pb(II) from aqueous solution onto Turkish kaolinite clay. *Journal of Hazardous Materials*, *149*, 283–291.

Septhum, A, Rattanaphani, A., Bremner, J. B., & Rattanaphani, V. (2007). An adsorption study of Al (III) ions onto chitosan. *Journal of Hazardous Materials*, *148*, 185–191.

Swayampakula, K., Boddu, V. M., Nadavala, S. K., & Abburi, K. (2009). Competitive adsorption of Cu(II), Co(II), and Ni(II) from their binary and tertiary aqueous solutions using chitosan-coated perlite beads as biosorbent. *Journal of Hazardous Materials*, *170*, 680–689.

Veera, M. B, Krishnaiah, A., Jonathan, L. T., & Edgar, D. S. (2003). Removal of hexavalent chromium from wastewater using new composite chitosan biosorbent. *Environmental Science and Technology*, *37*(19), 4449–4456.

Vijaya, Y., Popuri, S., Boddu, V., & Krishnaiah, A. (2008). Modified chitosan and calcium alginate biopolymer sorbents for removal of nickel (II) through adsorption. *Carbohydrate Polymers*, *72*, 261–271.

Virjayaghavan, K., Teo, T. T., Balasubramanian, R., & Joshi, U. M. (2009). Application of Sargassum biomass to remove heavy metal ions from synthetic multi-metal solutions and urban storm water runoff. *Journal of Hazardous Materials*, *164*, 1019–1023.

Wan, M. W., Petrisor, I. G., Lai, H. T., Kim, D., & Yen, T. F. (2004). Copper adsorption through chitosan immobilized on sand to demonstrate the feasibility for in situ decontamination. *Carbohydrate Polymers*, *55*, 249–254.

Wan, M., Kan, C. C., Rogel, B. D., & Dalida, M. L. P. (2010). Adsorption of copper (II) and lead (II) ions from aqueous solution on chitosan-coated sand. *Carbohydrates Polymers*, *80*, 891–899.

Wang, L., & Wang, A. (2008). Adsorption behaviors of Congo red on the N,O-carboxymethyl-chitosan/montmorillonite nanocomposite. *Chemical Engineering Journal*, *143*, 43–50.